nature portfolio

https://doi.org/10.1038/s41586-025-09106-8

Supplementary information

Brain implantation of soft bioelectronics via embryonic development

In the format provided by the authors and unedited

Supplementary discussion

Choosing PFPE-DMA with a molecular weight of 8 kDa. We chose the 8 kDa PFPE-DMA based on the fabrication yield. To increase the adhesion between the Au layer and the PFPE-DMA layer during Au deposition. We developed a new protocol that treats the PFPE-DMA surface with inert gas plasma, and then uses sputtering to deposit the Au layer. However, the sputtered Au layer was difficult to lift off. Our findings showed that a device made of softer PFPE-DMA had a lower overall lift-off yield, with yields of PFPE-DMA with molecular weights of 4-, 8-, 10-, and 12-kDa being around 95%, 90%, 70%, and 30%, respectively. As the result, we decided to choose 8 kDa PFPE-DMA, which has both sufficient softness and fabrication yield.

Face-down electrodes. During implantation, the electrodes are attached to an embryo, with their bottom side in contact with the neural plate (**Supplementary Fig. 1a**). Therefore, to enable signal recording after implantation, we developed a fabrication protocol to expose the electrodes to the bottom of the device, ensuring direct contact with the neural plate. In addtion, conventional SU-8 electronics utilized SU-8 as a back layer for the I/O pad. However, PFPE-DMA, being too soft, would beak during flip-chip bonding if still used as the back layer. Therefore, we designed the I/O pads on the silicon oxide substrate without the bottom passivation layer (**Supplementary Fig. 1b**).

Long-term rearing of cyborg tadpoles to cyborg frogs. We housed 11 cyborg tadpoles and 19 control tadpoles under the same conditions. At 40 days post fertilization, 5 cyborg tadpoles and 10 control tadpoles developed to stages 45–50, 3 cyborg tadpoles and 4 control tadpoles developed to stages 51–59, and 1 cyborg tadpole and 1 control tadpole developed to stages 60–65. 2 cyborg tadpoles and 4 control tadpoles died during this period. Although more control tadpoles died in

absolute number, due to the larger control group size, the survival rate was similar between the two groups (81.82% for cyborgs vs. 78.95% for controls).

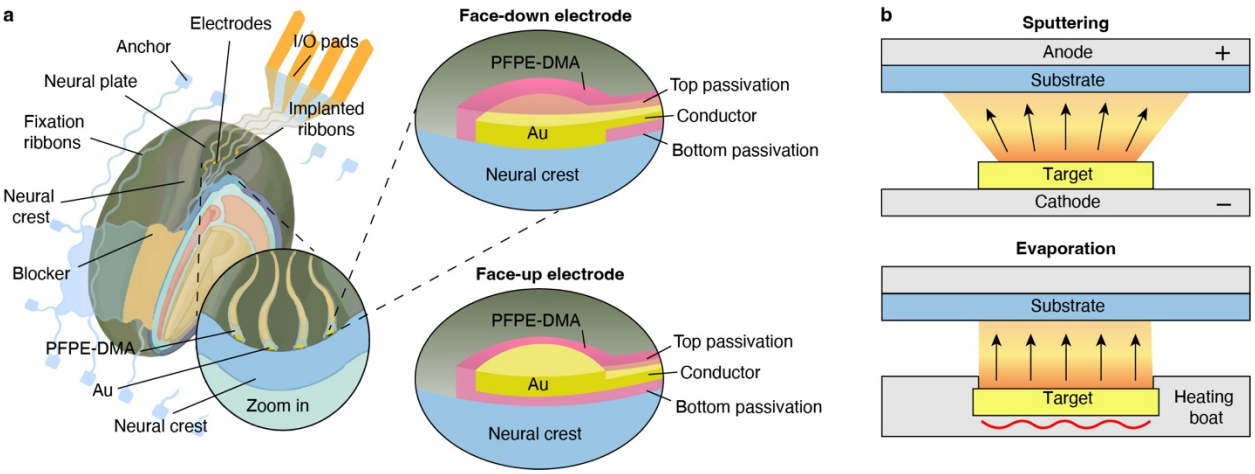

Supplementary Fig. 1 | Technical innovations critical to soft and stretchable PFPE-DMA mesh electronics. a, Schematics comparing face-up and face-down electrodes in soft and stretchable mesh electronics for embryo implantation and neural interfaces. **b,** Schematics showing sputtering (left) and evaporation (right) for metal deposition on PFPE-DMA layers.

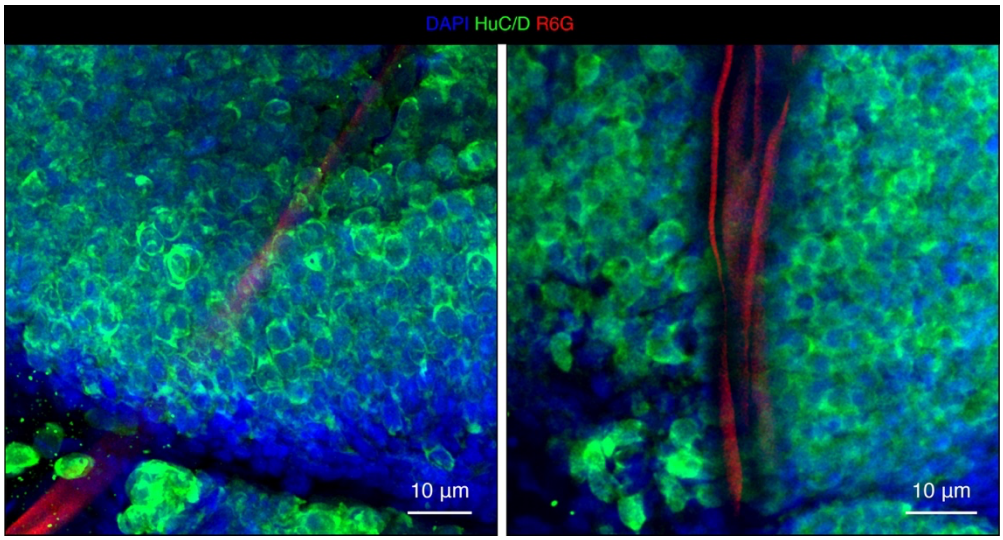

Supplementary Fig. 2 | Immunostaining images depicting the contact between *Xenopus* brain tissues and mesh electronics. Whole-mount-stained 3D reconstructed confocal fluorescence images of implanted mesh microelectronics showing the mesh embedded in the neural tissue. 4′,6-diamidino-2-phenylindole (DAPI) labels cell nuclei, HuC/D labels neurons, and Rhodamine 6G (R6G) labels the device. The experiment was repeated at least five times, yielding similar results.

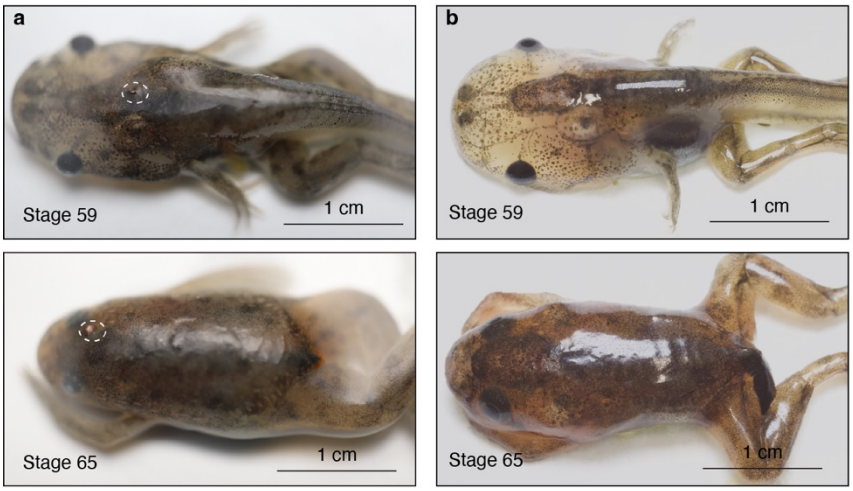

Supplementary Fig. 3 | Long-term rearing of cyborg tadpoles to cyborg frogs. a, Photos showing cyborg frogs at stage 59 (top) and stage 65 (bottom). Dashed circles highlight the interconnects of mesh electronics outside the brain. **b,** Photos showing control frogs at stage 59 (top) and stage 65 (bottom).

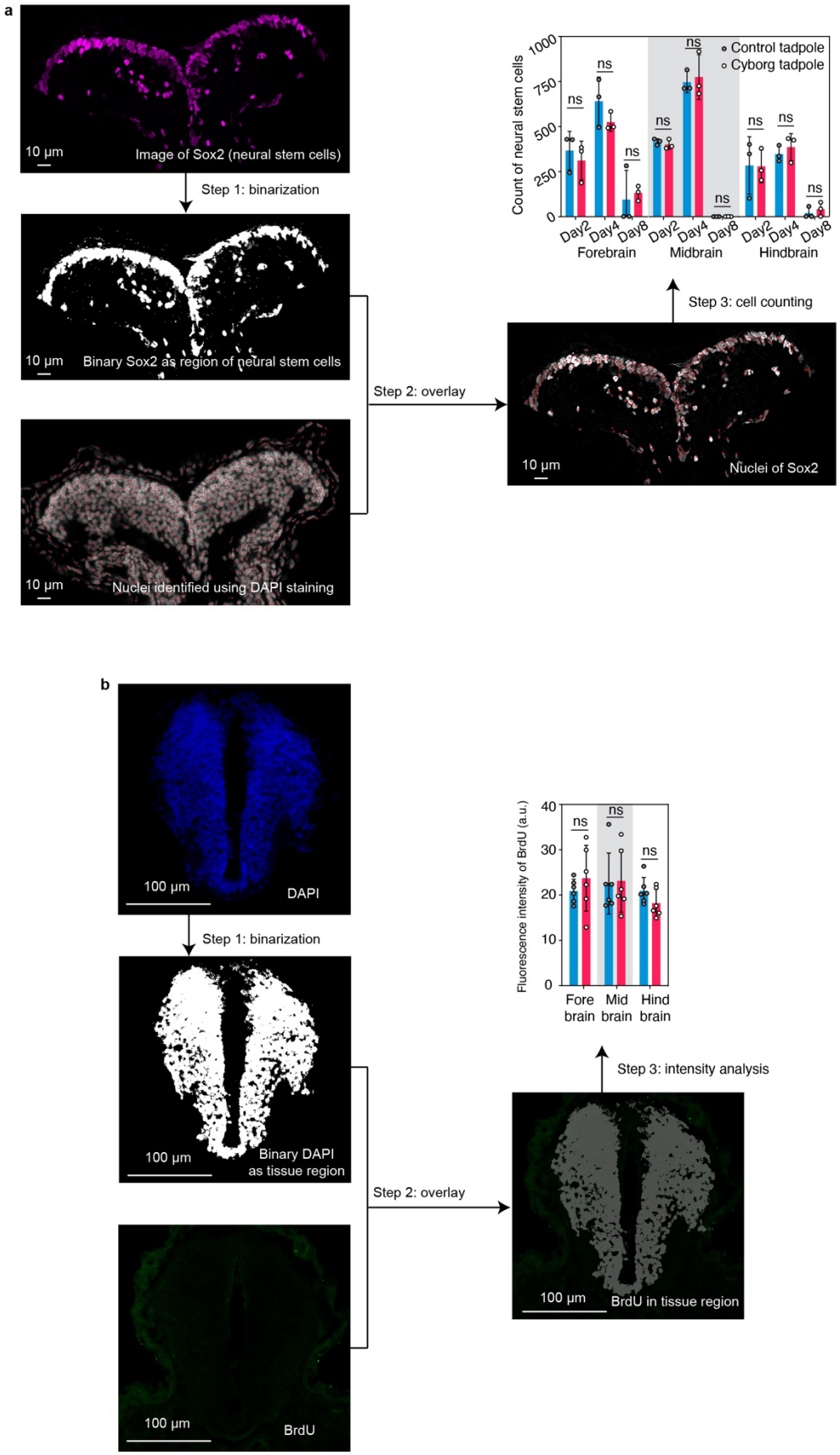
a
10 μm
Image of Sox2 (neural stem cells)
Step 1: binarization
10 μm
Binary Sox2 as region of neural stem cells
10 μm
Nuclei identified using DAPI staining
Step 2: overlay
10 μm
Nuclei of Sox2
Step 3: cell counting
Count of neural stem cells
Control tadpole
Cyborg tadpole
ns
Day2
Day4
Day8
Forebrain
Midbrain
Hindbrain
b
100 μm
DAPI
Step 1: binarization
100 μm
Binary DAPI as tissue region
100 μm
BrdU
Step 2: overlay
100 μm
BrdU in tissue region
Step 3: intensity analysis
Fluorescence intensity of BrdU (a.u.)
Fore brain
Mid brain
Hind brain

Supplementary Fig. 4 | Procedures for quantitative analysis of fluorescence images. a, Cell counting in SRY-box transcription factor 2 (Sox2, neuron stem cells) fluorescence images. First, the Sox2 image is binarized to identify the region of neuron stem cells (step 1). Then, the binary Sox2 image is overlaid with the DAPI-labeled cell nuclei to indicate the nucleus of neuron stem cells (step 2). Finally, the number of neuron stem cell nuclei is counted and reported (step 3, results are reported in **Fig. 3i**). **b,** Fluorescent intensity quantifying of bromodeoxyuridine (BrdU) images. First, the DAPI image is binarized to identify the tissue region (step 1). Then, the binary DAPI image is overlaid with the BrdU image (step 2). The fluorescent intensity of BrdU in the DAPI tissue region is calculated and reported (step 3, results are reported in **Fig. 3m**).

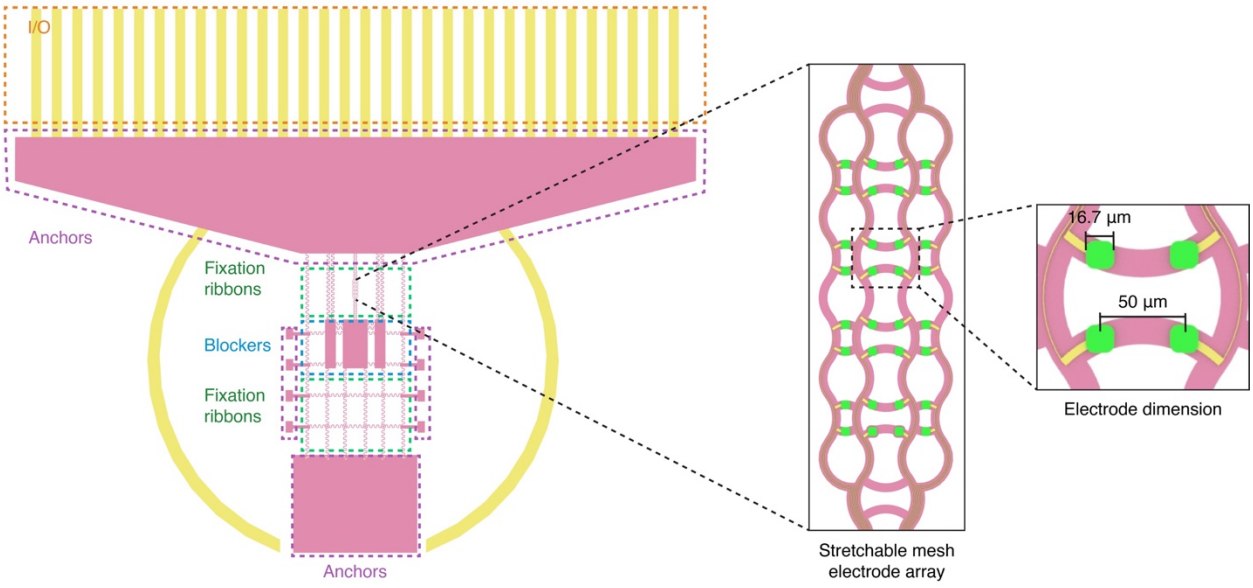

Supplementary Fig. 5 | Design of the stretchable mesh electronics with a 32-channel mesh electrode array. The design contains a high-density mesh electrode array, stretchable anchors and ribbons, and blockers for embryo integration.

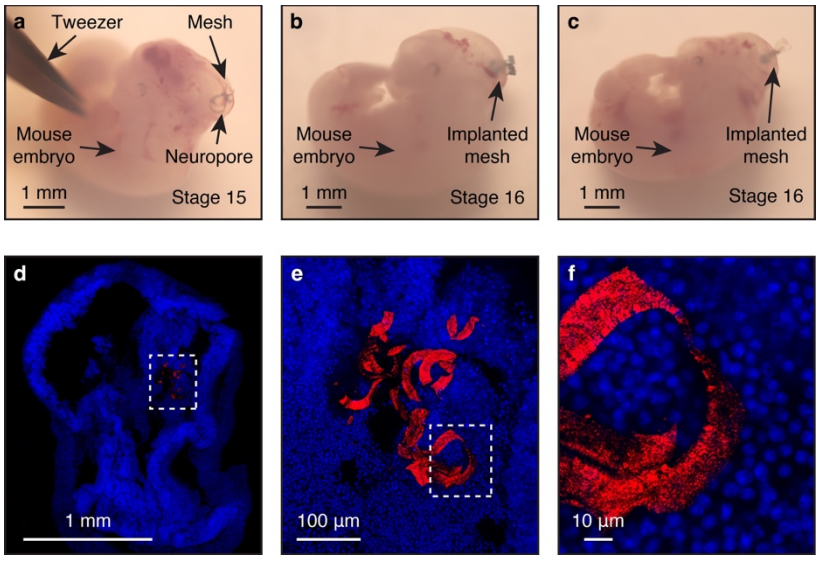

Supplementary Fig. 6 | Implantation of stretchable mesh electronics in mouse embryos. a-c, BF microscopic images showing three representative mouse embryos implanted with stretchable mesh electronics. **d,** Confocal fluorescence image showing coronal sections of a cyborg mouse embryo fixed at embryonic stage 16. Cell nuclei, blue, and mesh electronics, red (reflective mode). **e,** Zoomed-in view of the white dashed box-highlighted region in (**d**) showing the 3D integration of mesh electronics with the brain. **f,** Zoomed-in view of the white dashed box-highlighted region in (**e**) showing one stretchable ribbon. **d-f,** The experiment was repeated at least three times, yielding similar results.

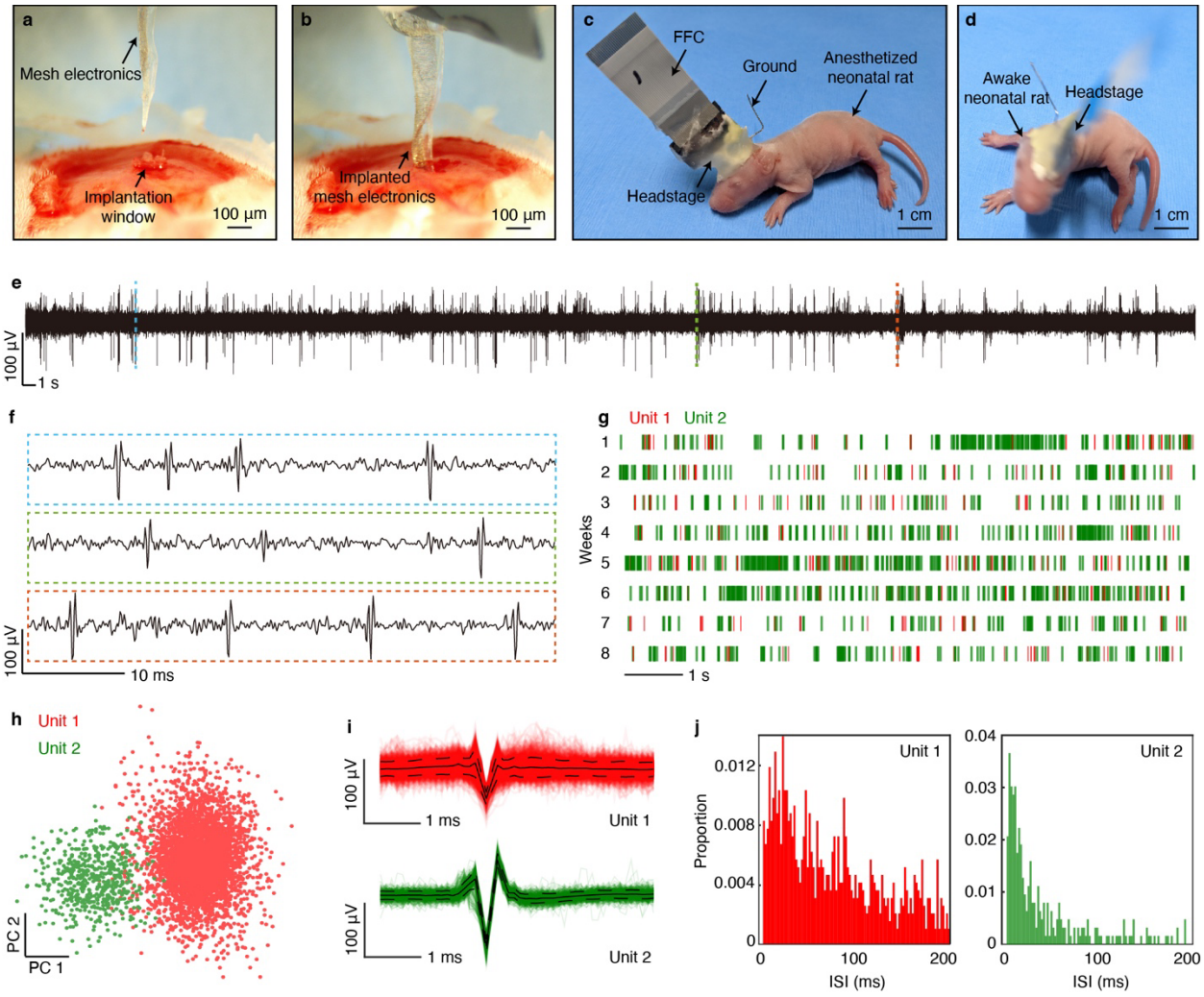

Supplementary Fig. 7 | Implantation of stretchable mesh electronics in neonatal rat brain. a, b, Photographic images showing mesh electronics before (**a**) and after (**b**) implantation into a neonatal rat brain. **c, d,** Photographic images showing the neonatal rat after stereotactic surgery (**c**) and after recovering from anesthetics (**d**). **e,** Representative filtered voltage traces (300-3,000 Hz bandpass filter) of neonatal rat at P12-14. **f,** Zoomed-in views of the signals highlighted by blue-, green- and red-dashed box-highlighted regions in (**e**). **g,** Raster plot of single-unit action potentials sorted from the recording. **h-j,** Principal component analysis (PCA) (**h**), average waveforms (mean ± s.d.) (**i**) and ISI (**j**) of two representative units.

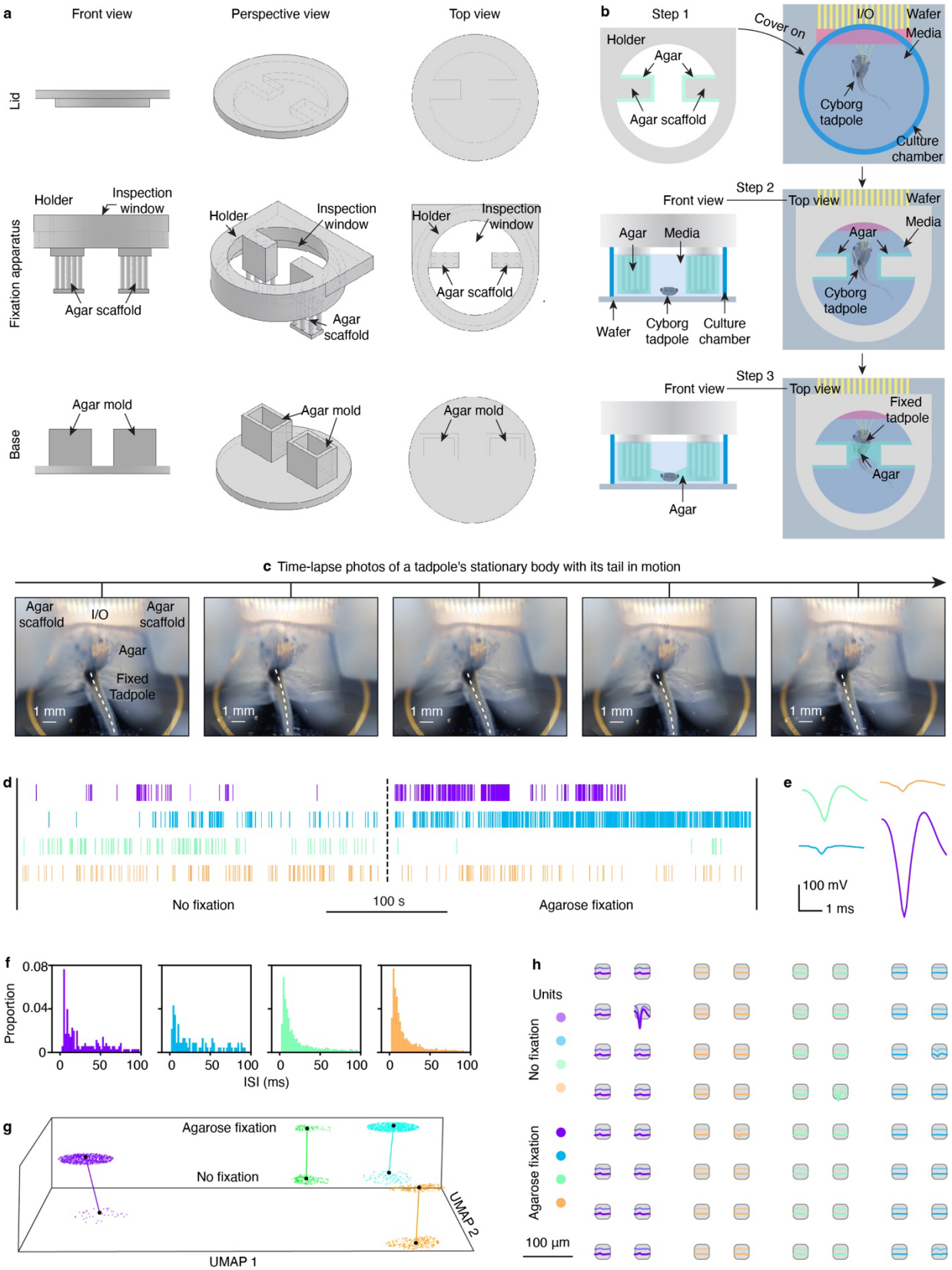
a
Front view
Perspective view
Top view
Lid
Fixation apparatus
Holder
Inspection window
Agar scaffold
Base
Agar mold
b
Step 1
Cover on
Holder
Agar
Agar scaffold
I/O
Wafer
Media
Cyborg tadpole
Culture chamber
Step 2
Front view
Top view
Agar
Media
Wafer
Cyborg tadpole
Culture chamber
Step 3
Fixed tadpole
c Time-lapse photos of a tadpole's stationary body with its tail in motion
Agar scaffold
I/O
Agar
Fixed Tadpole
1 mm
d
No fixation
100 s
Agarose fixation
e
100 mV
1 ms
f
Proportion
0.08
0.04
0
0
50
100
ISI (ms)
g
Agarose fixation
No fixation
UMAP 1
UMAP 2
h
Units
No fixation
Agarose fixation
100 µm

Supplementary Fig. 8 | Neural recording in awake cyborg tadpole. a, Front, perspective, and top views of the 3D-printed holder for the head-fixed recording. **b,** Schematics showing the stepwise fixation of the cyborg tadpole for awake recording. Step 1: A layer of agarose is cured on the agar scaffold of the holder. Step 2: The holder is placed on top of the culture chamber containing the anesthetized cyborg tadpole. The design of the holder ensures that the tadpole fits in the middle of the two agarose scaffolds. Step 3: A small amount of low melting point agarose further fixes the tadpole with the scaffolds. **c,** Time-lapse photographic images showing that in this setting, the tail of the agarose-fixed tadpole can still move during recording. **d,** Raster plot of spikes sorted from a representative recording of a cyborg tadpole with and without agarose fixation. **e, f,** Average waveforms (**e**) and ISI (**f**) of spikes sorted from recordings in (**d**). **g,** Uniform manifold approximation and projection (UMAP) analysis of neurons from recordings with and without agarose fixation. **h,** Representative average single-unit waveforms at each of the electrodes from recordings with and without agarose fixation. **d-h,** Each color corresponds to an identified unit.

Supplementary Table 1 | Actual p values in two-tailed unpaired t-tests

Fig. 2o											
Gelatin vs. Gelatin-device											
0.2875											
Fig. 3i, Cyborg tadpoles vs. Control tadpoles											
Forebrain				Midbrain				Hindbrain			
Day 2	Day 4	Day 8		Day 2	Day 4	Day 8		Day 2	Day 4	Day 8	
0.5621	0.2371	0.7246		0.4611	0.7422	0.3739		0.9670	0.4853	0.5032	
Fig. 3j, Cyborg tadpoles vs. Control tadpoles											
Forebrain				Midbrain				Hindbrain			
Day 2	Day 4	Day 8		Day 2	Day 4	Day 8		Day 2	Day 4	Day 8	
0.4468	0.9457	0.4194		0.2748	0.6646	0.1019		0.6379	0.6947	0.4875	
Fig. 3k								Fig. 3l			
Cyborg tadpoles vs. Control tadpoles								Cyborg tadpoles vs. Control tadpoles			
0.7542								0.2788			
Fig. 3m, Cyborg tadpoles vs. Control tadpoles											
Forebrain				Midbrain				Hindbrain			
0.3922				0.8845				0.1530			
Fig. 3n, Cyborg tadpoles vs. Control tadpoles											
apex2.L	*hsp70.L*	*hspd1.L*	*mapk1.L*	*piezo1.S*	*pif1.L*	*pds5b.L*	*plk1.S*	*pola1.S*	*rev1.S*	*tipin.L*	*xrcc1.L*
0.4244	0.3981	0.3767	0.2723	0.5017	0.3673	0.2498	0.7596	0.0568	0.4000	0.4502	0.9751
Fig. 3o, Cyborg tadpoles vs. Control tadpoles											
Day 4		Day 5		Day 6		Day 7		Day 8		Day 9	
Identical values		Identical values		0.7881		0.7581		0.9763		0.6593	
Fig. 3p, Cyborg tadpoles vs. Control tadpoles											
Day 4		Day 5		Day 6		Day 7		Day 8		Day 9	
Identical values		0.3559		0.8949		0.8912		0.5951		0.8784	
Fig. 3q, Cyborg tadpoles vs. Control tadpoles											
Day 4		Day 5		Day 6		Day 7		Day 8		Day 9	
Identical values		0.2544		0.9500		0.9048		0.0635		0.2500	
Fig. 3o, Comparison of developmental days				Fig. 3p, Comparison of developmental days				Fig. 3q, Comparison of developmental days			
Day 6 vs. Day 7				Day 6 vs. Day 7				Day 5 vs. Day 6			
< 0.0001				< 0.0001				< 0.0001			
Extended Data Fig. 4k											
Before vs. After stretching						Before vs. After bending					
0.6147						0.3459					
Extended Data Fig. 4o											
PFPE-DMA vs. Control						Degradation products vs. Control					
0.5793						0.2586					
Extended Data Fig. 8b											
No drug vs. APV/CNQX				APV/CNQX vs. Wash				Wash vs. APV/CNQX/TTX			
<0.0001				0.0004				0.0004			
Extended Data Fig. 8c											

No drug vs. APV/CNQX	APV/CNQX vs. Wash	Wash vs. APV/CNQX/TTX	
0.0343	0.0064	0.0024	
Extended Data Fig. 8g			
No drug vs. BIC/PTX	BIC/PTX vs. Wash	Wash vs. BIC/PTX/TTX	
0.0146	0.0202	0.0356	
Extended Data Fig. 8p			
Stage 24 vs. Stage 26	Stage 24 vs. Stage 40	Stage 26 vs. Stage 40	
< 0.0001	< 0.0001	< 0.0001	
Extended Data Fig. 8q			
Stage 24 vs. Stage 26	Stage 24 vs. Stage 40	Stage 26 vs. Stage 40	
0.0102	0.0003	0.0162	
Fig. 6h			
Day 1	Day 2	Day 3	Day 4
0.0105	0.0003	0.0249	0.2267
Extended Data Fig. 10c			
24 h vs 36 h			
< 0.0001			

Supplementary Table 2 | Primary and secondary antibodies

Name	Vendor	Catalog Number	Concentration
Recombinant Anti-HuD + HuC antibody	Abcam	AB184267	1:100
Anti-Acetylated Tubulin antibody, Mouse monoclonal	Sigma-Aldrich	T7451	1:100
BrdU Monoclonal Antibody (MoBU-1)	Invitrogen	B35128	1:100
Anti-SOX2 Monoclonal (Btjce)	Invitrogen	14-9811-82	1:100
Anti-Myt1/MTF1 antibody	Abcam	AB251682	1:100
Anti-vimentin antibody (SP20)	Abcam	AB16700	1:100
Ms mAb to ALDH1L1 (3E9)	Abcam	AB56777	1:100
Goat anti-Rat IgG (H+L) Cross-Adsorbed Secondary Antibody, Alexa Fluor™ 488	Invitrogen	A-11006	1:500
Goat anti-Rabbit IgG (H+L) Cross-Adsorbed Secondary Antibody, Alexa Fluor™ 594	Invitrogen	A-11012	1:500
IgG (H+L) Highly Cross-Adsorbed Donkey anti-Mouse, Alexa Fluor™ Plus 647	Invitrogen	A-32787	1:500
Goat anti-Rabbit IgG (H+L) Highly Cross-Adsorbed Secondary Antibody, Alexa Fluor™ Plus 488	Invitrogen	A-32731	1:500
Alexa Fluor™ 647 Phalloidin	Thermo Fisher SCIENTIFIC	A22287	1:50

Supplementary Table 3 | Yield of neurulation implantation

Embryo	Implantation	Survival	Recording [a]	Embryo	Implantation	Survival	Recording [a]
1	Success	Yes	32/32	2	Success	Yes	32/32
3	Success	Yes	31/32	4	Success	Yes	32/32
5	Success	Yes	32/32	6	Failure	N/A	N/A
7	Success	Yes	16/16	8	Success	Yes	14/16
9	Success	Yes	4/4	10	Failure	N/A	N/A
11	Success	Yes	4/4	12	Success	No	N/A
13	Success	Yes	4/4	14	Success	Yes	4/4
15	Success	Yes	N/A, mesh	16	Success	Yes	N/A, mesh
17	Success	Yes	N/A, mesh	18	Success	Yes	N/A, mesh
19	Failure	N/A	N/A	20	Success	Yes	N/A, mesh
21	Success	Yes	N/A, mesh	22	Success	Yes	N/A, mesh
23	Failure	N/A	N/A	24	Success	Yes	N/A, mesh
25	Success	Yes	N/A, mesh	26	Failure	N/A	N/A
27	Success	Yes	N/A, mesh	28	Success	Yes	N/A, mesh
29	Success	Yes	N/A, mesh	30	Success	Yes	N/A, mesh
31	Failure	N/A	N/A	32	Success	Yes	N/A, mesh
33	Success	Yes	N/A, mesh	34	Success	Yes	N/A, mesh
35	Success	Yes	N/A, mesh	36	Success	Yes	64/64
37	Success	Yes	63/64	38	Success	Yes	N/A, stimulation
39	Success	Yes	N/A, stimulation	40	Success	No	N/A
41	Success	Yes	N/A, stimulation	42	Success	Yes	N/A, stimulation
43	Success	Yes	N/A, stimulation	44	Success	Yes	N/A, stimulation
45	Success	Yes	N/A, stimulation	46	Success	Yes	N/A, stimulation
47	Success	Yes	N/A, stimulation	48	Success	Yes	N/A, stimulation

a, The recording column is reported as number of electrodes that have generated signals/ total number of electrodes. "mesh" refers to devices that have not been bonded with I/O for mechanical and behavioral tests.